UNIVERSITY OF OKLAHOMA

GRADUATE COLLEGE

LINEAR POST LINEAR FLOW PRODUCTION ANALYSIS

A THESIS

SUBMITTED TO THE GRADUATE FACULTY

in partial fulfillment of the requirements for the

Degree of

MASTER OF SCIENCE

By

TRENT BONE
Norman, Oklahoma
2017

LINEAR POST LINEAR FLOW PRODUCTION ANALYSIS

A THESIS APPROVED FOR THE
MEWBOURNE SCHOOL OF PETROLEUM AND GEOLOGICAL ENGINEERING

BY

_____
Dr. Jeffrey Callard, Chair

_____
Dr. Deepak Devegowda

_____
Dr. Mashhad Fahs

© Copyright by TRENT BONE 2017
All Rights Reserved.

To my family and friends.

Acknowledgements

I would like to thank the members of my thesis committee Dr. Jeffrey Callard, Dr. Deepak Devegowda, and Dr. Mashhad Fahs. A special thanks to my thesis advisor, Dr. Jeffrey Callard, for helping me further my education, as well for his continuous advice and direction throughout the past year.

I also want to thank OU, specifically the Mewbourne School of Petroleum and Geological Engineering for giving me the opportunity and tools to pursue a master degree in petroleum engineering.

I would also like to acknowledge student work during the 2017 Senior Capstone course, Integrated Reservoir Management, for eliciting the predominance of the linear post linear flow regime in the provinces cited and for providing the Bakken well example used in Fig. 2.

Lastly, I would like to thank my family and friends for the motivation and support while I took on this task.

Table of Contents

List of Figures

Abstract

This study was motivated by the production data observed from multi-fractured horizontal wells in the field that have two infinite acting flow regimes. These two infinite acting flow regimes appear as two straight lines on a plot of cumulative production versus the square root of produced time. This phenomenon has been coined *linear post linear flow*, and it appears to be the most prominent flow regime in various plays including the Permian Basin, Eagle Ford Shale, Bakken Shale, and the SCOOP and STACK plays of Oklahoma.

The objectives of this study were to reproduce field production responses of linear post linear flow through numerical simulation, and to develop a model for forecasting production in such cases. To accomplish these goals numerical simulations representing an element of symmetry along a multi-fractured horizontal well containing three fractures were run with varying fracture spacing and length. The simulations were successful in predicting linear post linear flow.

Chapter 1: Introduction and Literature Review

Chapter 1 gives some background information and explains the reason why this study was conducted. The first section provides background information necessary to understand the need for this research; the second section discusses some of the previous research conducted that will be utilized during this study; and the final section outlines the organization of this work.

1.1 Overview of this Research

This study focuses on the analysis of production data on a cumulative production versus square root of time plot. Traditionally, there has been two flow regimes in multi-fractured horizontals, infinite acting and boundary dominated, depicted in Figure 1.

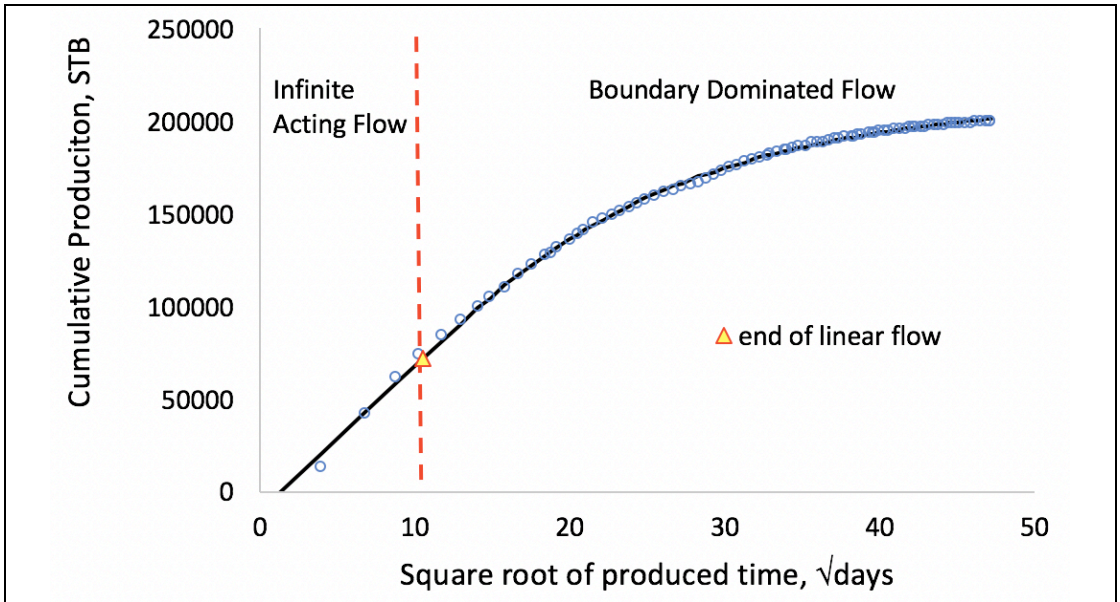

Figure 1. Cumulative production versus square root of time showing the infinite acting and boundary dominated flow periods of the Carbon Valley 25 Federal Com 4H in the Wolfcamp formation, Eddy County, New Mexico from Bone (2017).

As multi-fractured horizontals mature and more production data becomes available a new production response has been observed that has two linear infinite acting regimes,

the initial infinite acting flow followed by another linear flow with a depressed slope, Figure 2. This phenomenon has been coined linear-post-linear flow.

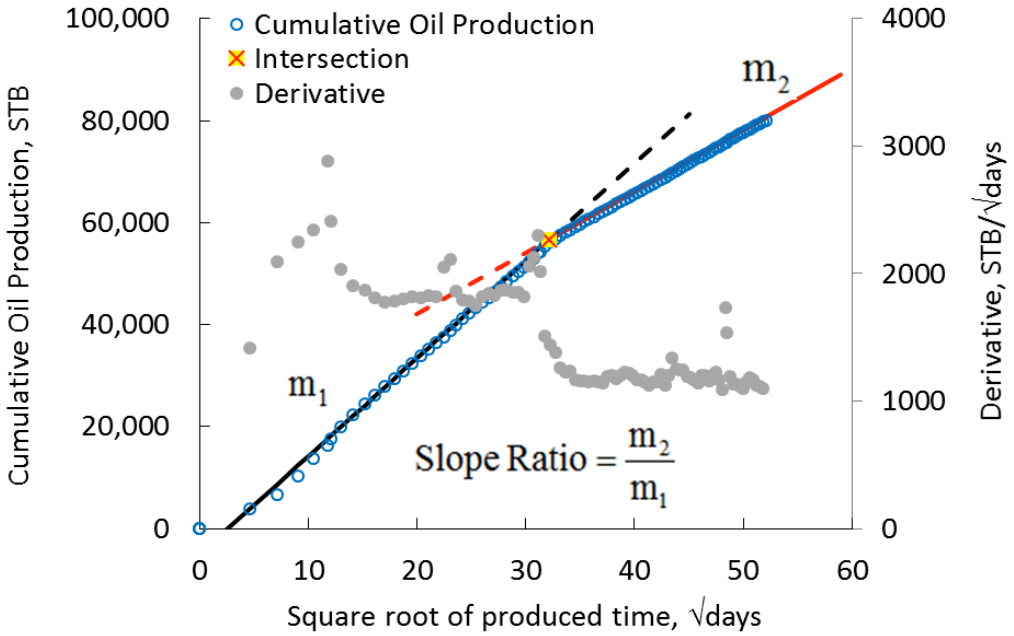

Figure 2. Cumulative production versus square root of time showing linear post linear flow of the Flint Chips 5H in the Bakken formation, Dunn County, North Dakota from Bone (2017).

The goal of this research is to determine why this linear-post-linear phenomenon occurs using numerical simulation of multi-fractured horizontals with varying fracture lengths and spacing, as well as the implications of the flow regime for production forecasting and reserve determination.

1.2 Literature Review

This work utilizes production analysis with a cumulative production versus square root of produced time plot. This method was briefly suggested by Wattenbarger et al. (1998), and was employed by Rodrigues and Callard (2012). A straight line is fit to the data during the infinite acting flow, and then at the time of end of linear flow a curve is generated to fit the boundary dominated data using an Arps (1956) hyperbolic forecast. In the cases of linear post linear flow, Childers (2016) discusses a method to forecast

production that he employed evaluating the Bakken Shale in McKenzie County, North Dakota. First, the infinite acting and semi-infinite acting flow data are fit with two separate straight lines, m_1 and m_2 in Figure 2. Then the semi-infinite acting flow data is forecasted using m_2 until an economic limit or an assumed 40-year casing life is reached. This method over predicts ultimate recovery for linear post linear wells because it assumes boundary dominated flow will not occur in the life of the well. One aim of this thesis was to improve this forecasting method to obtain more reliable recoveries for linear post linear wells.

Childers (2016) also discusses methods for stochastically forecasting production for wells that remain in infinite acting flow. The first step is to determine the flow regimes for all wells in the area being evaluated. The wells should be categorized into linear flow (infinite acting flow), boundary dominated flow, and linear post linear flow (semi-infinite acting flow). To forecast wells probabilistically the mature wells in the area being evaluated must be forecasted first. Once all the boundary dominated wells are forecasted the Arps exponents and time to end of linear flow must be collected from them. Additionally, the linear post linear wells must be forecasted, and the intersection time (the point in time the flow transitions from infinite acting to semi-infinite acting flow, denoted as a yellow box with a red X in Figure 2) along with the production slope ratio (the ratio of m_2 to m_1) should be gathered for all wells. In the cases of boundary dominated flow a probabilistic profile for the Arps exponent and the time to end of linear flow should be generated based on the collected data, and for the cases of linear post linear flow the same should be done for the production slope ratio and the intersection time. When that is completed Monte Carlo simulation can be used on wells

that are still in infinite acting flow. Initially, the flow regime distribution between linear post linear flow and boundary dominated flow, mentioned previously, should be randomly sampled to determine what flow regime a well in infinite acting flow is predicted to enter. Following, if the predicted flow is boundary dominated then sampling from the probabilistic profiles created are used to determine when a well is likely to enter boundary dominated flow and to what degree it will decline, or if the predicted flow is linear post linear flow then the same is done for the intersection time and production slope ratio. This process is iterated through with increasing realizations and the average ultimate recovery across all realizations is averaged for each well until convergence on a solution for ultimate recovery is obtained, Figure 3 below illustrates the Monte Carlo convergence for a multi-fractured horizontal in the Bakken. This process is described in detail by Childers (2016) in the Bakken Shale for McKenzie County, North Dakota.

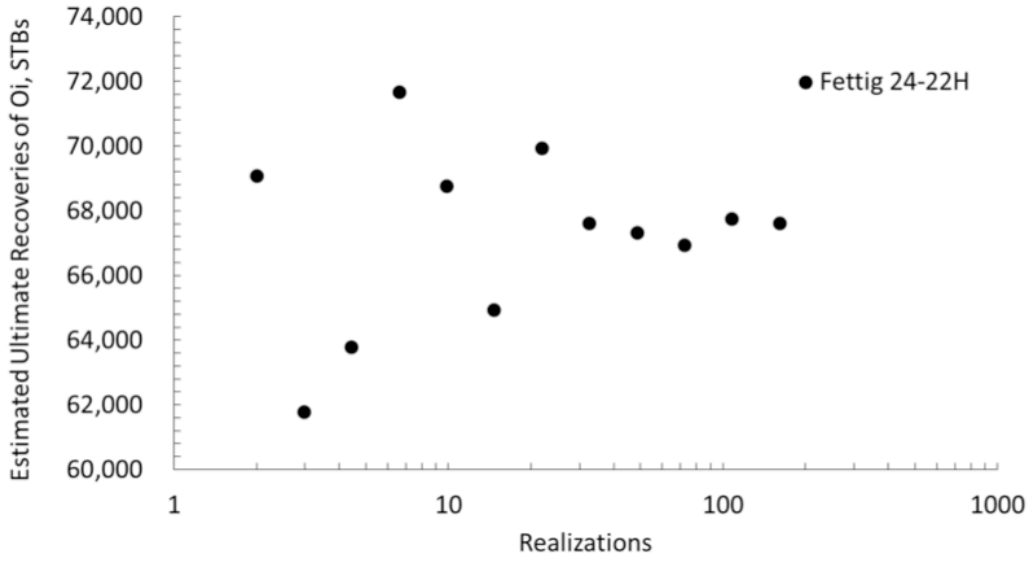

Figure 3. Monte Carlo simulation for and Estimated Ultimate Recovery of Oil, Fettig 24-22H McKenzie County, North Dakota from Childers (2016).

1.3 Thesis Organization

The chapters of this thesis are organized in an order of how the work was accomplished. First, the models used in the simulations are described. The simulation formulation is followed by the resulting data, and then the utilization of the results is discussed.

Chapter 2 discusses the format of the simulation models used in this study.

Chapter 3 discusses the analysis and findings of the simulations.

Chapter 4 discusses the utilization of the results in forecasting production and estimating reserves.

Chapter 5 summarizes the findings of this work and discusses what can be done in the future concerning linear post linear flow.

Appendix A shows the resulting data in table format and the methods used in analyzing the production data.

Appendix B has an example of an Eclipse input file used in this study, and a visual representation of one of the simulations in Eclipse.

Appendix C reviews the simulation models created that were not able to achieve linear post linear flow.

Chapter 2: Simulation Preparation

2.1 Grid Format

The numerical simulations for this study were done using Eclipse™ reservoir simulator. A two-dimensional grid was used in the simulations to represent a single stage of a horizontal well with three hydraulic fractures to represent an element of symmetry, shown in Figure 4 below. The grid was created in such a way that the dimensions of the grid blocks increased logarithmically from all fractures and wellbores, a visual is provided in Appendix B.2. This was done to capture the near wellbore/fracture effects. Two variables were manipulated separately in the simulations to determine the cause of linear-post-linear flow, varying fracture spacing and varying fracture length.

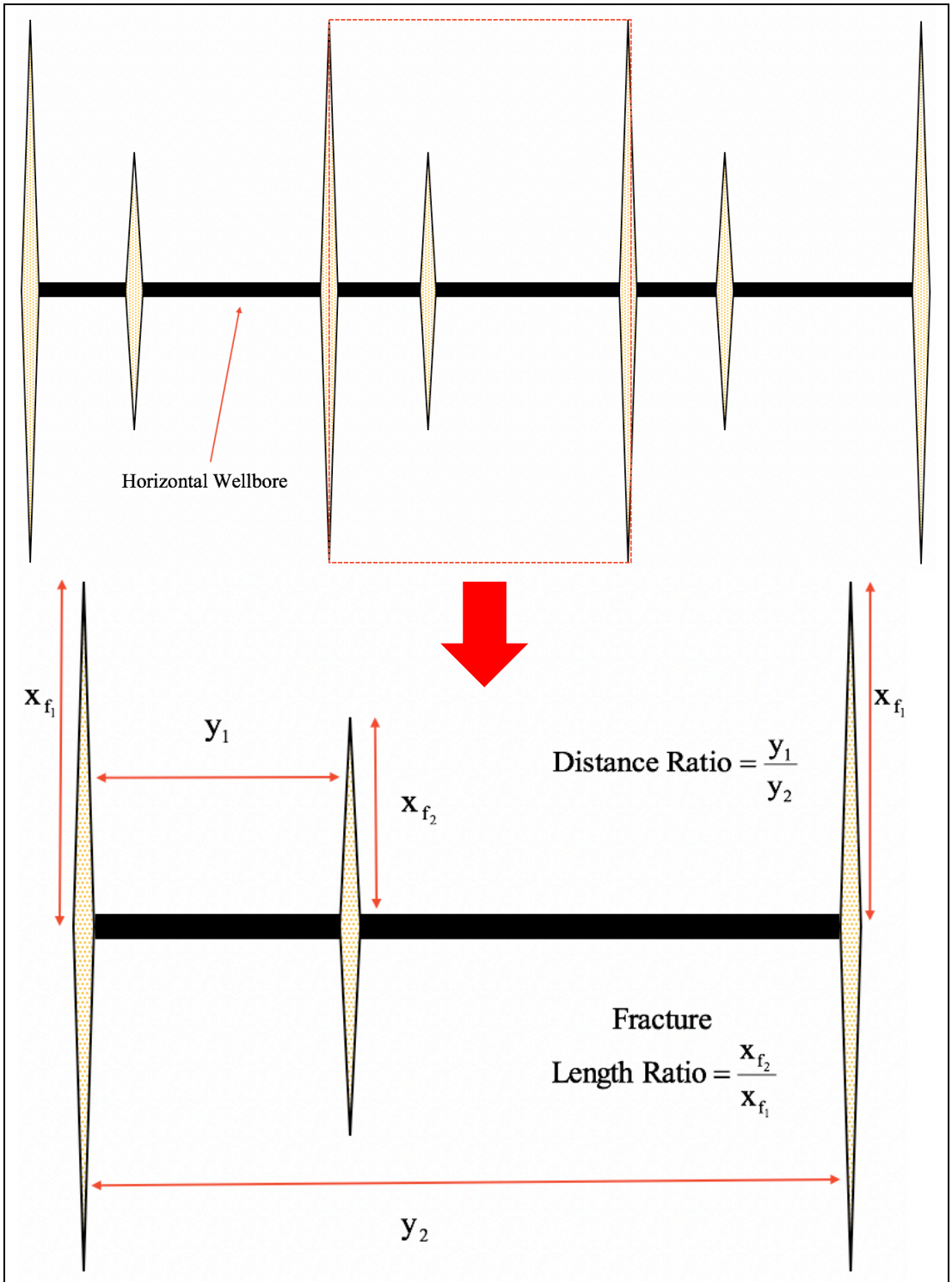

Figure 4. Plan view of multi-stage horizontal well and element of symmetry from Bone (2017).

2.2 Reservoir Properties

The fluid type used in the simulations had small but constant compressibility. Additionally, the initial reservoir pressure was 5000 psi and the reservoir porosity and permeability had nominal values. Ultimately, the conclusions of this study are independent of reservoir properties and purely dependent on the fracture geometry. The three fractures in the simulations were created by changing the permeability of the grid blocks containing the fractures so that it would be equivalent to a dimensionless fracture conductivity of 500.

2.3 Well Information

Three wells were placed in the first row of grid blocks along the longest edge in line with each fracture. The wells produced at a constant bottom hole pressure of 4500 psi and the production data for all wells were added together to simulate one horizontal wellbore.

2.4 Varying Fracture Length

One of the two variables manipulated in this study was the fracture length. The two outer fractures had equal length for all simulations. The middle fracture's length was varied relative to the outer fractures. This variation is described by the term *fracture length ratio*, which is the ratio of the outer fracture length to the inner fracture length. The fracture length ratio varied from 10% to 100%.

2.5 Varying Fracture Spacing

The other variable manipulated was fracture spacing. The term *distance ratio* is used to describe the variation in fracture spacing. The distance ratio is the ratio of the distance between the middle fracture and the nearest adjacent fracture with the distance between

the outer fractures. For every variation of fracture length five cases of varying distance ratios were run with distance ratios varying from 10% to 50%. Note that a distance ratio of 50% is equidistant from the adjacent fractures.

Chapter 3: Results

Before presenting the results, it should be noted that while the models used in this study were successful in reproducing production data observed in the field other models may also have similar results.

3.1 Varying Fracture Length Ratio

In the cases of linear post linear flow observed in the field, the production data has slope ratio's ranging from 0.5 to 1. In 2016 Childers did a study for probabilistically forecasting ultimate recovery in which he analyzed the distribution of the linear post linear production slope ratios in McKenzie County in the Bakken Shale, Figure 5 shows a normal distribution presentation.

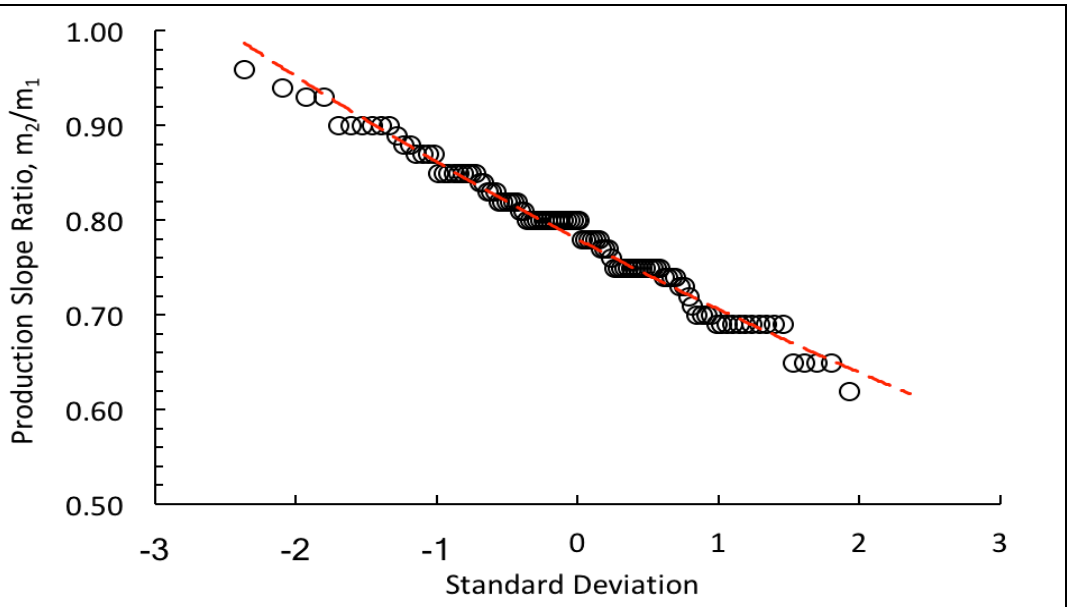

Figure 5. Distribution of production slope ratios for 110 wells in the Bakken Shale, McKenzie County from Childers (2016).

All the production slope ratios in Childers study are within the range of 0.5 to 1, and this range of slope ratio's is repeatable by using the models described in chapter 2. The logarithmic relationship between the production slope ratio and fracture length ratio is shown in Figure 6. The inset figure in Figure 5 depicts a scenario where the distance

ratio is 30%, but the relationship is consistent for all distance ratios except for 50%. The relationship fails at a distance ratio of 50% because the fractures are all evenly spaced which results in a typical infinite acting flow and then boundary dominated flow scenario. The results of the simulations indicate that production slope ratio is independent of the distance ratio and only affected by the fracture length ratio. The curve in Figure 5 may not be useful, but it validates the model used in this study because field observations were able to be replicated.

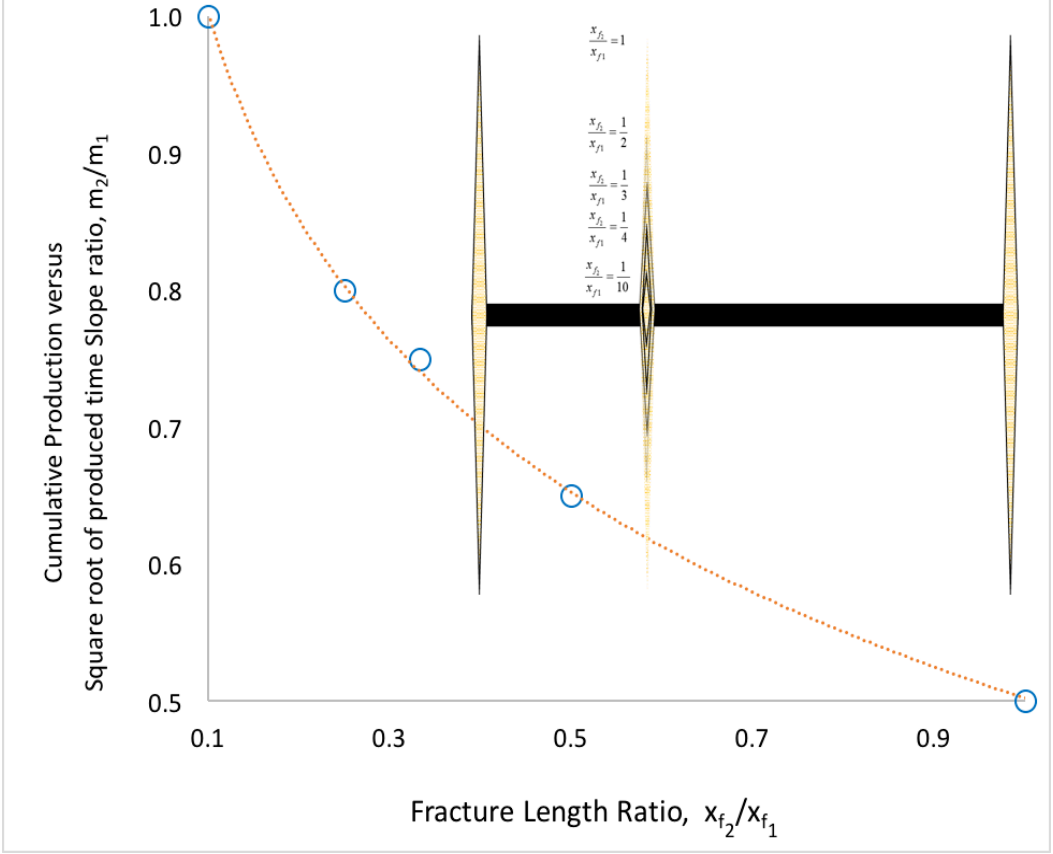

Figure 6. Relating the production slope ratio to fracture length ratio for $y_1/y_2 < 0.5$ from Bone (2017).

3.2 Varying Fracture Distance Ratio

Linear post linear multi-fractured horizontals go from infinite acting flow to semi-infinite acting flow and then following that, transition into boundary dominated flow

(according to simulations). The time at which these flow regime changes occur is dependent upon the location of the fractures. The time at which boundary-dominated flow began and the time of intersection of the linear flows were taken from the simulations described in chapter 2 to compute a time ratio. The yellow square with a red X and the yellow triangle in Figure 7 below are the intersection time and the time boundary dominated flow begins.

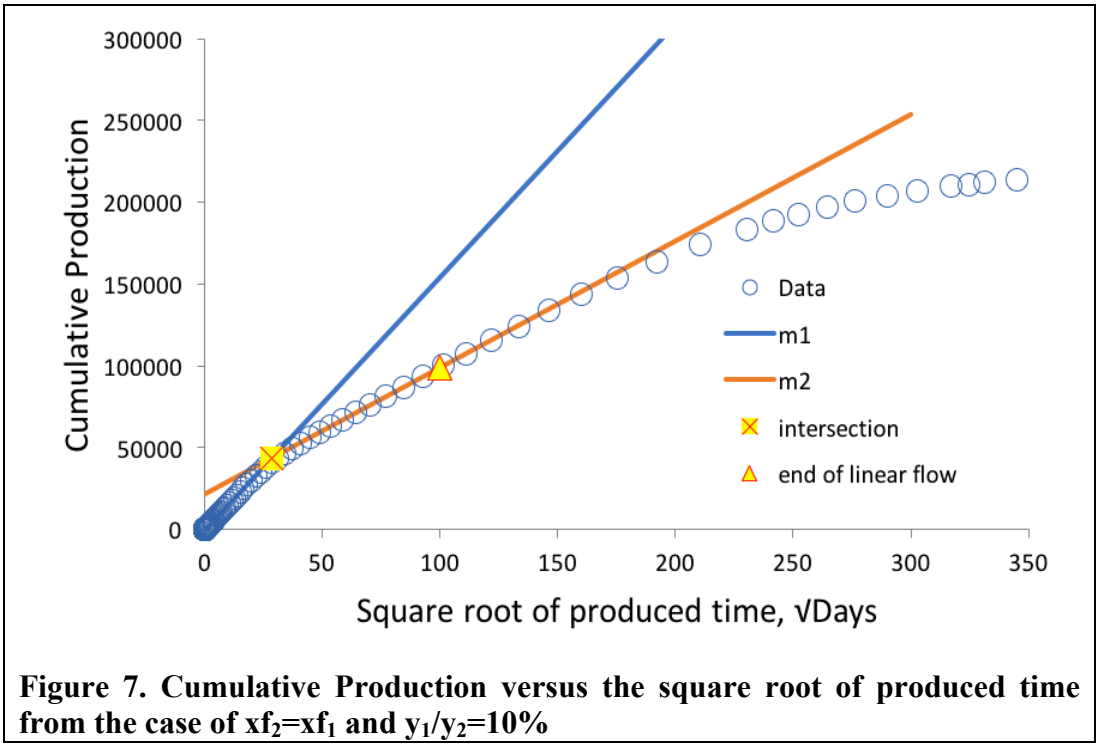

Figure 7. Cumulative Production versus the square root of produced time from the case of $xf_2=xf_1$ and $y_1/y_2=10\%$

These time ratios were plotted versus the standard deviation assuming equal probability of each geometry occurring, depicted in Figure 8 with an inset figure of the varying distance ratios annotated on the plot. The inset figure only depicts a fracture length ratio of 0.5, but all fracture length cases are plotted.

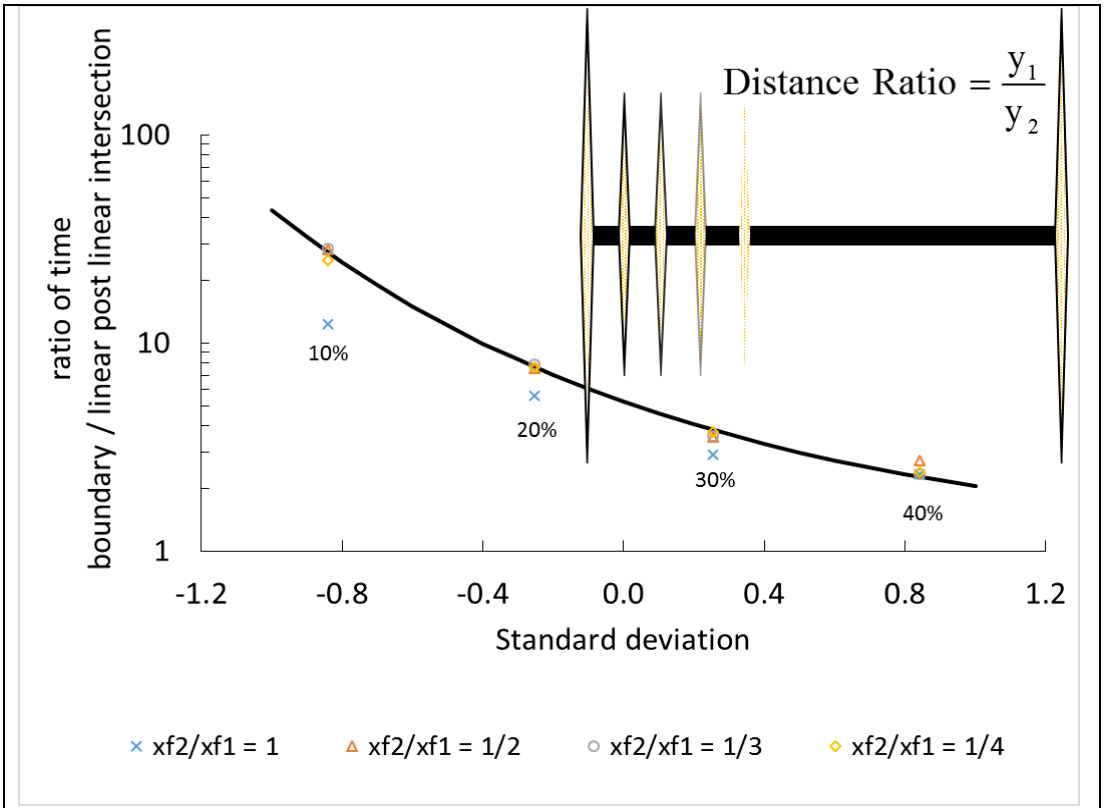

Figure 8. Production analysis of varying fracture height (legend code) and varying distance ratio from 10% to 40% demonstrating the time to boundary dominated flow as a ratio of the time of linear post linear intersection time from Bone (2017).

The time ratios for the cases with equal fracture length for all fractures fall well below the curve fit, but for all other cases with unequal fracture length the data points are tightly grouped. The curve fit is generated with all points except for the cases with all fractures having equal length. This result suggests that the times at which the flow regimes transition are independent of the fracture length ratio, while the position of the fractures strongly affect these times.

Chapter 4: Reserve Determination

For wells that are in boundary dominated flow the Arps (1956) equations can be used to forecast production and deterministically estimate reserves, but for wells that are in infinite acting (linear) or semi-infinite acting (linear post linear) flow the reserves cannot be estimated deterministically. Figure 9 illustrates flow regime distribution data collected from the University of Oklahoma class, Integrated Reservoir Management, where students must evaluate the reserves in a specific area.

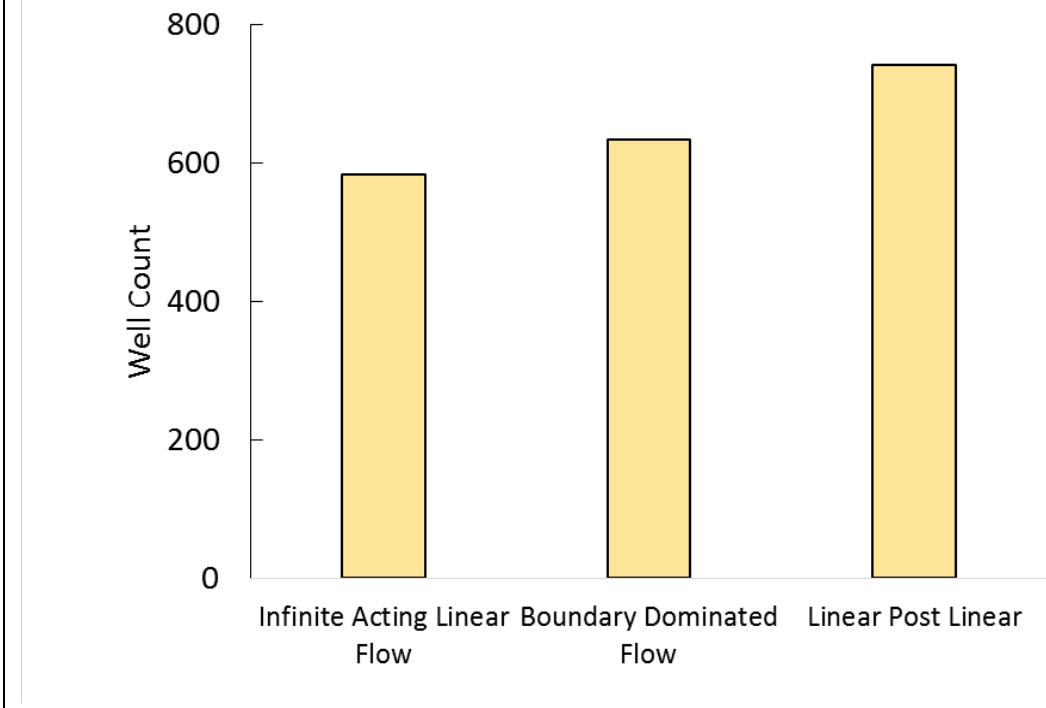

Figure 9. Distribution of current flow regimes from New Mexico, North Dakota, Oklahoma and Texas Unconventional Plays from Bone (2017).

4.1 Stochastic Determination of Reserves

As depicted above about two thirds of wells require stochastic methods to estimate reserves. This is based on the probability that a multi-fractured horizontal will enter either boundary dominated flow or linear post linear flow following the infinite acting flow regime. For the cases where linear post linear flow is the probable next flow

regime Figure 8 should be used by iterating through random sampling to approximate the end of linear flow and the onset of boundary dominated flow. Once wells mature and linear post linear wells begin to enter boundary dominated flow in the field, those observations can be used to make more reliable predictions.

Chapter 5: Conclusions

5.1 Conclusions

This study was successful in reproducing linear post linear flow field responses, as well as offering a simple method for forecasting production. Ultimately the conclusions reached concerning the linear post linear flow phenomenon are:

1. Model validation of unequal and irregular spaced fractures creating linear post linear flow was substantiated with the range of slope ratios observed in the field.
2. The end of the *linear post linear* flow is determined by the fracture distance ratio and independent of the fracture length ratio.

It should be noted that this work represents a simple model that reproduces production trends that have been observed in the field. Other models may also be able to replicate these observations, only when wells mature will predictions become more dependable.

5.2 Future Work

As wells mature many linear post linear wells will have entered boundary dominated flow and the podium plot in Figure 8 will have an additional column stating the well count of linear post linear boundary dominated wells. The production for linear post linear boundary dominated wells will be able to be deterministically forecasted using the Arps (1956) hyperbolic forecast. Additionally, the simulated data in Figure 7 will be able to be replaced with observed field data, and linear post linear wells that have not entered boundary dominated flow will be probabilistically forecasted using Monte Carlo simulation with more reliable data.

References

Arps, J.J. ; *Estimation of Primary Oil Reserves*, 1956, presented at the Petroleum Conference – Economics and Evaluation, Dallas, Texas, 29-30 March 1956

Bone, T., Devegowda, D., and Callard, J. 2017, *Linear Post Linear Flow Production Analysis*, URTeC 2697518, Unconventional Reservoir Technology Conference, Austin, Texas, 24-26 July 2017

Childers, David. 2016, *Forecasting Ultimate Recovery Using Probabilistic Model for Flow-Regime Changes*, Master Thesis, University of Oklahoma.

Rodrigues, E. S., and Callard, J. G. 2012, *Permeability and Completion Efficiency Determination From Production Data In the Haynesville, Eagle Ford and Avalon Shales*, SPE – 161335, SPE Eastern Regional Meeting held in Lexington, Kentucky, USA, 3–5 October 2012

Wattenbarger, R.A., El-Banbi, A.H., Villegas, M.E. and Maggard, J.B. 1998, *Production Analysis of Linear Flow into Fractured Tight Gas Wells*, SPE 39931, SPE Rocky Mountain/Regional Low Permeability Symposium and Exhibition, Denver, Colorado, 5-8 April 1998

Appendix A: Nomenclature

$\frac{m_2}{m_1}$ Slope ratio of two straight lines observed in cumulative production versus square root of produced time, dimensionless

STB Stock Tank Barrel

$\frac{x_{f_2}}{x_{f_1}}$ Fracture half-length ratio, dimensionless

$\frac{y_2}{y_1}$ Fracture distance ratio, dimensionless

SCOOP South Central Oklahoma Oil Province

STACK Sooner Trend Anadarko Basin Canadian and Kingfisher Counties

Appendix B: Simulation Data

B.1 Data used throughout this work.

Table B1. Resulting data of all simulations discussed in this work.

% Distance	x_{f2}/x_{f1}	m_2/m_1	$\sqrt{t_x}$	√telf	$\sqrt{t_{elf}}/\sqrt{t_x}$
10%	1	0.50	28.5	100	3.51
20%	1	0.50	57	135	2.37
30%	1	0.50	82	140	1.71
40%	1	0.50	98	150	1.53
10%	0.5	0.65	33	175	5.30
20%	0.5	0.65	60	165	2.75
30%	0.5	0.65	85	160	1.88
40%	0.5	0.65	100	165	1.65
10%	0.33	0.75	31	165	5.32
20%	0.33	0.75	57	160	2.81
30%	0.33	0.75	82	155	1.89
40%	0.33	0.75	100	153	1.53
10%	0.25	0.80	33	165	5.00
20%	0.25	0.80	58	160	2.76
30%	0.25	0.80	83	160	1.93
40%	0.25	0.80	100	155	1.55
10%	0.1	1.00	145	145	1

B.2 Determination of production slope ratio and time ratio

To determine the production slope ratios and time ratios accurately and precisely a method other than calculating the slope across a range of data was needed. Calculating the slope across a range of data would not be precise because the exact portions of the data to fit each line were unknown. This lack of precision would result in approximate slopes that were not ideal for calculating slope ratios consistently across all the simulations.

A difference method was employed that involved calculating the production using the equation of a line and then subtracting that number from the actual simulation production data. The slope and intercept used in the line equation would be manipulated until a portion of the data was level set at zero. A result of zero would indicate the proper slope fit to the correct portion of the data. Figure B1 shows this method for finding the proper slope for the m_1 line and Figure B2 shows the same for the m_2 line. The point after the difference points become non-zero is the time selected for the flow regime transitions.

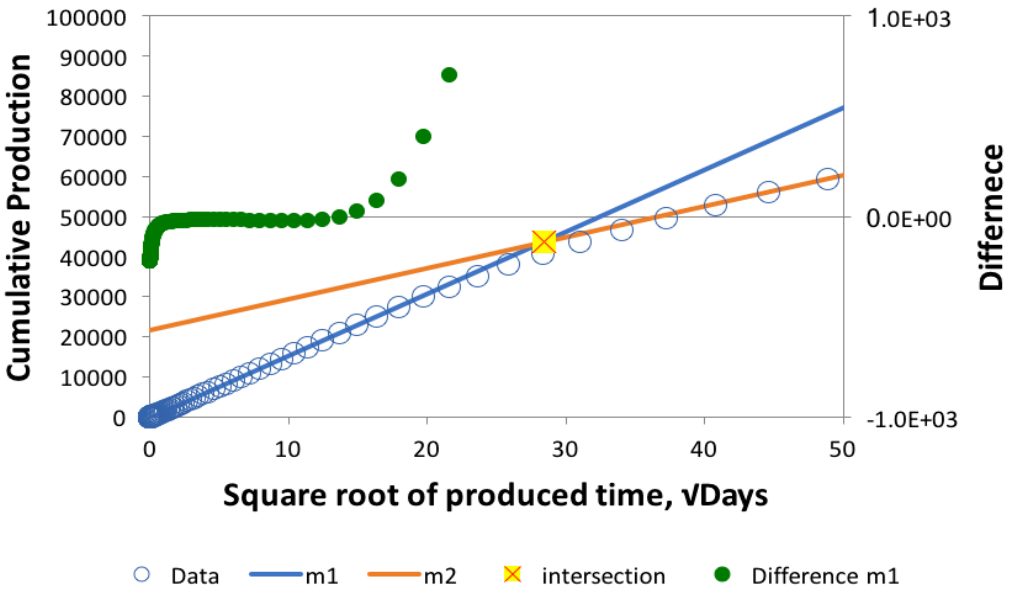

Figure B1. Example of simulation production data and determination of m_1 and intersection time for case of fracture length ratio of 1 and distance ratio of 10%.

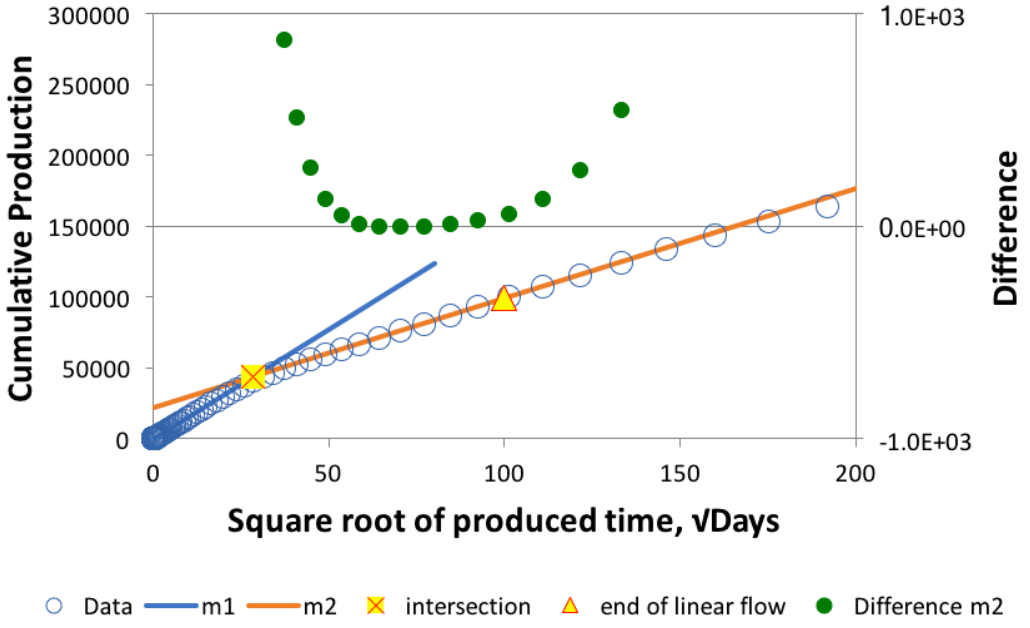

Figure B2. Example of simulation production data and determination of m_2 and time of end of linear flow for case of fracture length ratio of 1 and distance ratio of 10%.

Appendix C: Simulation Preparation

C.1 Example of input file for reservoir simulator

```
-- CfD 500
-- March 6, 2017
-- Line Source yeD=10
-- Constant Pressure 4500 psia
--Water
NOECHO

RUNSPEC
=========================================================================

TITLE
 Vertical fracture model, (Wf)r=0.5 in ==> (Wf)e=2 ft


DIMENS
---- dx   dy   dz
    21   84  1  /

-- Fluid phases present
WATER


-- Units
FIELD

--length of stack used by linear solver
NSTACK
  50  /

------------ #wells,  # connections,  #groups,  #wells per group
WELLDIMS
             3          1            1            3  /

-- Start simulation date
START
  1  JAN  1997 /

-- run to be restarted from unified restart file
UNIFIN

-- Restart and summary files written are to be unified
UNIFOUT

GRID
=========================================================================

TOPS
1764*4950/

DXV
-- reservoir

-- half fracture-1
2 4 8 16 32 64 128 6*256 128 64 32 16 8 4 2 2044
-- well
/
```

```
DYV

2.00  2.54  3.24  4.12  5.24  6.66  8.48  10.78 13.72 17.45 22.20 28.24 35.92 45.70 58.13
73.95 94.08 119.68  152.24  193.67  246.37  193.67  152.24  119.68  94.08 73.95 58.13 45.70
35.92 28.24 22.20 17.45 13.72 10.78 8.48  6.66  5.24  4.12  3.24  2.54  2.00  1.57  2.00
2.90  4.21  6.10  8.84  12.82 18.60 26.97 39.10 56.71 82.23 119.24  172.91  250.74  363.61
527.27  764.59  1108.74 1607.80 2331.48 3380.89 2331.48 1607.80 1108.74 764.59  527.27
363.61  250.74  172.91  119.24  82.23 56.71 39.10 26.97 18.60 12.82 8.84  6.10  4.21  2.90
2.00  1.38

/

DZ
1764*100
 /

EQUALS
  PERMX    0.1          1  21  1   84  1  1 / -- reservoir X permeability
  PORO     0.2          1  21  1   84  1  1 / -- reservoir Porosity
--CfD 500
    PERMX    51075      1  21  1   1   1  1 / -- equivalent fracture X
    PORO     0.0073     1  21  1   1   1  1 / -- equivalent fracture X porosity
/

--SECOND FRACTURE

EQUALS
--CfD 500
    PERMX    51075      1  20  42   42   1  1 / -- equivalent fracture X
    PORO     0.0073     1  20  42  42   1  1 / -- equivalent fracture X porosity
/


--THIRD FRACTURE

EQUALS
--CfD 500
    PERMX    51075      1  21  84   84   1  1 / -- equivalent fracture X

  PORO     0.0073      1  21  84   84   1  1 / -- equivalent fracture X porosity
/

----- Symmetry on X -----

MULTIPLY
  PERMX    0.5          1   1   1   41  1  1 /
  PORO     0.5          1   1   1   41  1  1 /
/

MULTIPLY
  PERMX    0.5          1   1   43   84  1  1 /
  PORO     0.5          1   1   43   84  1  1 /
/
----- Symmetry on Y ----- (symmetry through well-bores and fracture)

--Frac 1
MULTIPLY
  PERMX    0.5          1  21  1   1  1  1 /
  PORO     0.5          1  21  1   1  1  1 /
/
```

```
--Frac 2
MULTIPLY
 PERMX   0.5         1  20  42   42  1  1 /
 PORO    0.5         1  20  42   42  1  1 /
/

--Frac 3
MULTIPLY
 PERMX   0.5         1  21  84   84  1  1 /
 PORO    0.5         1  21  84   84  1  1 /
/

COPY
 PERMX   PERMY      1 21 1  84  1  1 /
 PERMX   PERMZ      1 21 1  84  1  1 /
/

Multiply
 PERMX   0         1 21 2  41  1  1/
 PERMX   0   1 21 43  83  1  1/
/

INIT

GRIDFILE
 0 1 /

RPTGRID
 TRANX TRANY /

PROPS
================================================================================


PVTW
-- PREF   BW(PREF)   CW    VW(PREF)   CVW
  5000.0   1.015    3.0D-6    1.0      0
/

ROCK
-- PREF     CR
  5000.0    0
/

DENSITY
-- OIL   WATER   GAS
  44.09  62.28  0.066 /

RPTPROPS
/

SOLUTION
================================================================================

--   DATUM DATUM  OWC    OWC    GOC    GOC   RSVD  RVVD  SOLN
--   DEPTH PRESS DEPTH   PCOW  DEPTH   PCOG  TABLE TABLE  METH
EQUIL
     5000   5000    1*    1*    1*    1*    1*     1*    1*   /


RPTSOL
-- Fluid       Create init
```

```
-- in place     Restart file
   FIP=1        RESTART=2  /

RPTRST
 BASIC=2 /

SUMMARY
=============================================================================

-- Well quantities
-- Well BHP
WBHP
/
-- Well water production rate
WWPR
/

-- Field Average Pressure
FPR

FWPT

FWIP


RUNSUM
EXCEL


SCHEDULE
=============================================================================

RPTRST
 BASIC=2 /

RPTSCHED
 WELSPECS /

WELSPECS
-- WELL GROUP  -LOCATION-   BHP  PHASE DRAINAGE FLAG  FLAG  FLAG  PRESS FLAG
-- NAME NAME    I   J     DEPTH       RADIUS   GAS  SHUT  CROSS TABLE DENS
   W1    G1    1   1       1*   WATER   1*      STD   SHUT   NO    1*    SEG  /
   W2    G1    1   42      1*   WATER   1*      STD   SHUT   NO    1*    SEG  /
   W3    G1    1   84      1*   WATER   1*      STD   SHUT   NO    1*    SEG  /
/

COMPDAT
-- WELL --LOCATION--   OPEN/   SAT  CONN  WELL   EFF  SKIN    D    PENETRATION
-- NAME   I  J  K1  K2  SHUT   TAB  FACT  DIAM   KH  FACTOR FACTOR  DIRECTION
   W1   1  1   1  1   OPEN   1*   1*   0.60   1*    0      0       Z   /
   W2   1  42  1  1   OPEN   1*   1*   0.60   1*    0      0       Z   /
   W3   1  84  1  1   OPEN   1*   1*   0.60   1*    0      0       Z   /
/


WCONPROD
-- WELL  OPEN/  CNTL  OIL  WATER GAS  LIQU  RES  BHP  THP   VFP   ALQ
-- NAME  SHUT   MODE  RATE RATE  RATE RATE  RATE         TABLE
   W1   OPEN   BHP  1*    1*   1*   1*    1*   4500   1*    1*    1*  /
   W2   OPEN   BHP  1*    1*   1*   1*    1*   4500   1*    1*    1*  /
   W3   OPEN   BHP  1*    1*   1*   1*    1*   4500   1*    1*    1*  /
 /
```

```
TUNING
 -- TSINIT  TSMAXZ  TSMINZ  TSMCHP  TSFMAX  TSFMIN  TSFCNV TFDIFF THRUPT --
       1       9000 /
--    0.1   0.15       3       0.3       0.1   1.25 1E20/
-- NEWTMX NEWTMN LITMAX LITMIN MXWSIT MWPIT DDPLIM --
--    12     1    25     1     8     8    4*1E6/
/
/

TSTEP
1.46E-07      2.91E-08      3.49E-08      4.19E-08      5.03E-08      6.04E-08
7.24E-08      8.69E-08      1.04E-07      1.25E-07      1.50E-07      1.80E-07
2.16E-07      2.60E-07      3.11E-07      3.74E-07      4.48E-07      5.38E-07
6.46E-07      7.75E-07      9.30E-07      1.12E-06      1.34E-06      1.61E-06
1.93E-06      2.31E-06      2.78E-06      3.33E-06      4.00E-06      4.80E-06
5.76E-06      6.91E-06      8.29E-06      9.95E-06      1.19E-05      1.43E-05
1.72E-05      2.06E-05      2.48E-05      2.97E-05      3.63E-05      4.28E-05
5.13E-05      6.16E-05      7.39E-05      8.87E-05      1.06E-04      1.28E-04
1.53E-04      1.84E-04      2.21E-04      2.65E-04      3.18E-04      3.84E-04
4.58E-04      5.49E-04      6.59E-04      7.91E-04      9.49E-04      1.14E-03
1.37E-03      1.64E-03      1.97E-03      2.36E-03      2.83E-03      3.40E-03
4.08E-03      4.90E-03      5.88E-03      7.05E-03      8.46E-03      1.02E-02
1.22E-02      1.46E-02      1.75E-02      2.10E-02      2.53E-02      3.03E-02
3.64E-02      4.37E-02      5.24E-02      6.29E-02      7.55E-02      9.05E-02
1.09E-01      1.31E-01      1.63E-01      1.88E-01      2.25E-01      2.70E-01
3.24E-01      3.89E-01      4.67E-01      5.61E-01      6.73E-01      8.07E-01
9.69E-01      1.16E+00      1.39E+00      1.67E+00      2.01E+00      2.41E+00
2.89E+00      3.47E+00      4.17E+00      5.00E+00      6.00E+00      7.20E+00
8.64E+00      1.04E+01      1.25E+01      1.50E+01      1.79E+01      2.15E+01
2.58E+01      3.10E+01      3.71E+01      4.46E+01      5.35E+01      6.84E+01
7.70E+01      9.24E+01      1.11E+02      1.33E+02      1.60E+02      1.92E+02
2.30E+02      2.76E+02      3.31E+02      3.97E+02      4.77E+02      5.72E+02
6.87E+02      8.24E+02      9.89E+02      1.19E+03      1.43E+03      1.71E+03
2.06E+03      2.47E+03      2.96E+03      3.55E+03      4.26E+03      5.12E+03
6.14E+03      7.37E+03      8.84E+03      1.06E+04      1.27E+04      1.53E+04
/
TUNING
 -- TSINIT  TSMAXZ
       9000    9000 /
/
/
TSTEP
1.83E+04      2.19E+04      2.76E+04      3.16E+04      3.79E+04      4.55E+04
5.46E+04      6.55E+04      7.86E+04      9.44E+04      1.13E+05      1.36E+05
1.76E+05      1.96E+05      2.35E+05      2.82E+05      3.38E+05      4.06E+05
--4.87E+05
--5.85E+05     7.02E+05
--     8.84E+05       1.01E+06       1.21E+06/

/
```

Figure C1. Input file for case of fracture length ratio of 0.5 and distance ratio of 10%.

C.2 Simulation Grid Example

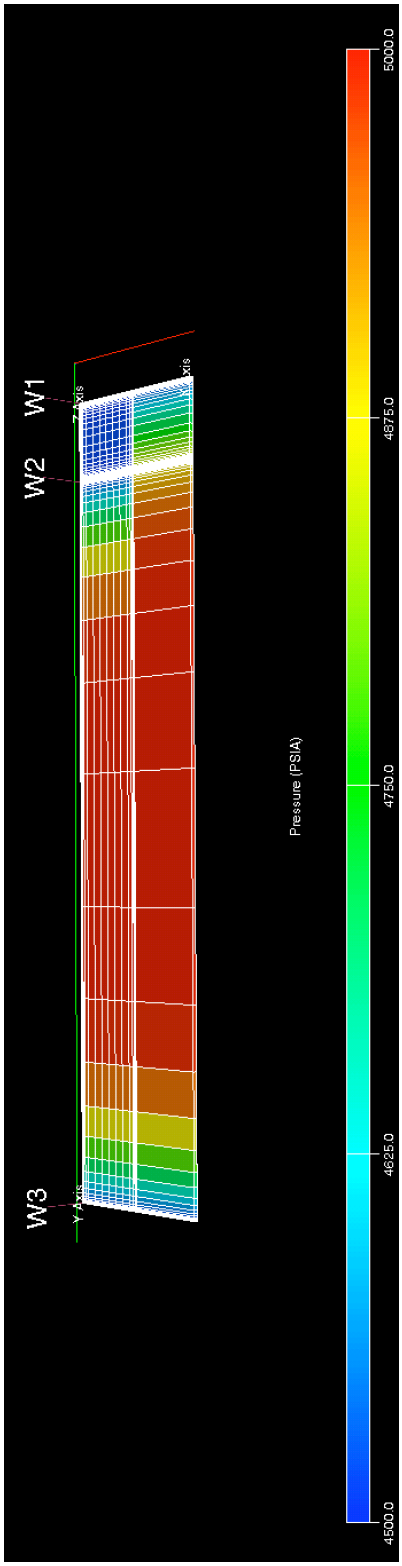

Figure C2. Simulation grid partially run of case with fracture length ratio of 0.5 and distance ratio of 10%.

Appendix D: Process

D.1 Varying Only Fracture Length

The initial approach for this study only considered a variation in fracture length as the cause for linear post linear flow. To test this hypothesis a nearly identical grid described in Chapter 2 was used. The simulation grid used in these runs only differed in that there were only two fractures, instead of three, on the edges of the grid with wells located on the edge of each fracture. A schematic of this grid layout is provided below in Figure D.1.

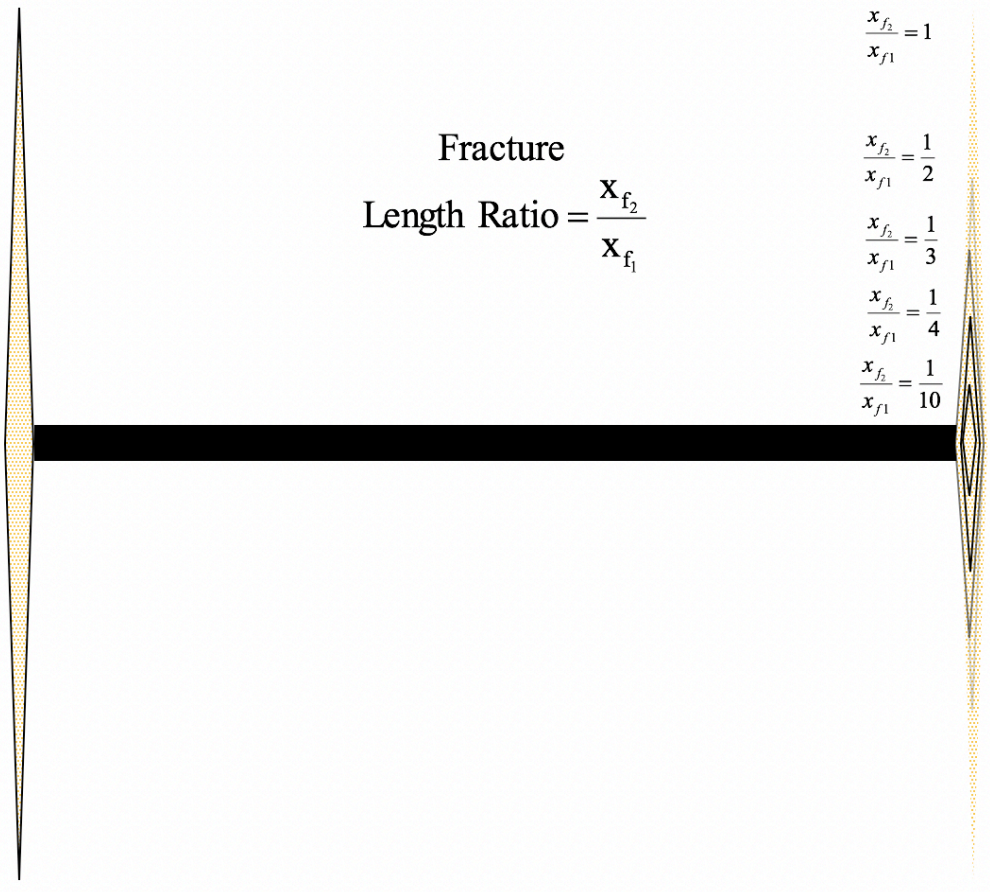

Figure D1. Schematic of the simulations run with two fractures only varying fracture length ratio.

It was hypothesized that semi-infinite acting flow would occur when the pressure fronts met in the middle due to the partial penetration of one of the fractures. A visualization of this scenario has been provided in Figure D2. Ultimately this grid format for simulations was unsuccessful in achieving linear post linear flow and only resulted in a typical infinite acting flow transitioning into boundary dominated flow scenario similar to that depicted in Figure 1 in Chapter 1.

Figure D2. Simulation grid partially run of case with fracture length ratio of 0.5 with only two fractures on the edges of the grid.

D.2 Varying Only Fracture Spacing

Following the failure to achieve linear post linear flow with varying fracture length the next grid format tested the effect of uneven fracture spacing. At this point to simplify the simulations various grids were made of different sizes but with the same fracture lengths and then the different simulations were added together in assorted pairs. It was later realized that this procedure resulted in a portion of flow that was missing when the simulations were added together in this manner, but it ultimately led to the final format used in this study. Figure D.3 shows an illustration of the grid format. One simulation contained everything to the right of the red dashed line and another simulation contained everything to the left of the dashed red line to the boundary represented by the black dashed line and the production from each was added together on the same time steps.

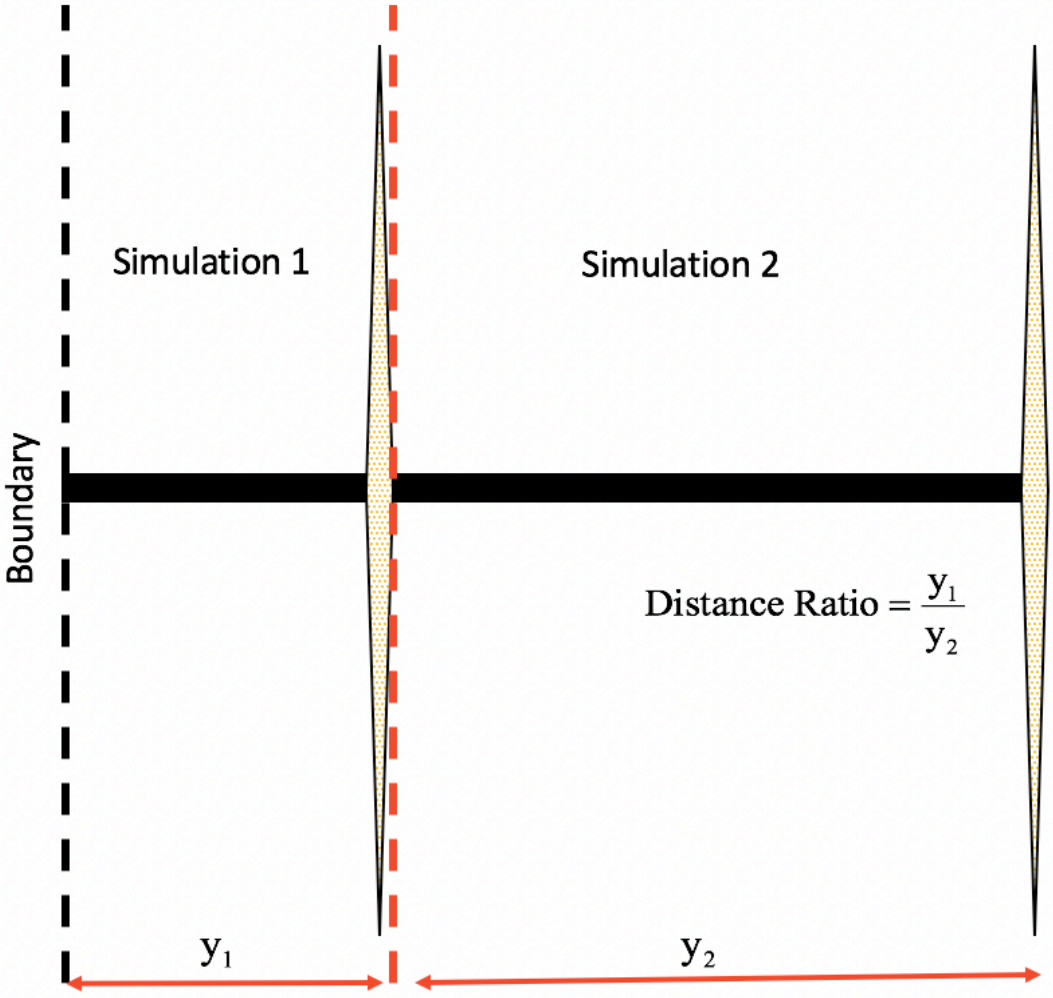

Figure D3. Schematic of the simulations run with two fractures only varying distance ratio.

Several combinations were run and all resulted in linear post linear flow, but the only production slope ratio across all the simulations were 0.5. It was obvious that there was another variable required to obtain the results observed in the field of the production slope ratio varying from 0.5 to 1. Additionally, at this point it was realized that adding the simulations together in this manner resulted in a non-physical result because it missed out on the crossover flow after the pressure fronts would meet at the no flow

boundary in between the fractures. These realizations resulted in the grid formats described in Chapter 2.